Histol Histopathol (2025) 40: 523-540

Histology and Histopathology
From Cell Biology to Tissue Engineering

ORIGINAL ARTICLE Open Access

SIRT4 is associated with microvascular infiltration, immune cell infiltration, and epithelial mesenchymal transition in hepatocellular carcinoma

Juan Li[1], Ming Zhao[2], Weiwei Fan[3,4], Na Na[1], Hui Chen[5], Ming Liang[3], Sheng Tai[6] and Shan Yu[1]

[1]Department of Pathology, The Second Affiliated Hospital of Harbin Medical University, Harbin, [2]Department of Gastroenterology, Clinical Medical College and the First Affiliated Hospital of Chengdu Medical College, Sichuan, [3]Department of Infectious Diseases, The Second Affiliated Hospital of Harbin Medical University, [4]Department of Infectious Medicine, Heilongjiang Provincial Hospital, [5]Department of Finance, Harbin Finance University and [6]Department of General Surgery, The Second Affiliated Hospital of Harbin Medical University, Harbin, PR China

Summary. Aims. Hepatocellular carcinoma (HCC) is the third leading cause of cancer death worldwide. In the present study, we evaluated SIRT4 expression levels in HCC specimens and investigated the relationships between SIRT4 expression levels, clinicopathological factors, and microvascular infiltration (MVI) in HCC.

Methods. The expression levels of SIRT4 in 108 HCC specimens were examined by immunohistochemical staining. MVI in HCC specimens was divided into three subtypes: M0, M1, and M2. Comprehensive bioinformatics analysis was carried out to demonstrate SIRT4's biological functions and expression-related prognostic value.

Results. The diffuse cytoplasmic expression pattern of SIRT4 was observed in all adjacent nonneoplastic liver tissues. The levels of SIRT4 were higher in HCC than in any other type of cancer and normal tissues. In addition, the expression levels of SIRT4 were significantly decreased in HCC tissues when MVI was M1 or M2 (P=0.003) but were not related to the overall clinical outcome. To explain MVI regulated by SIRT4, we also found that SIRT4 expression correlated with epithelial-mesenchymal transition (EMT) markers and CD4+ T/NK cells and downregulated cancer-associated fibroblast cells. Also, there was a significant relationship between MVI and degree of cell differentiation (P=0.003), tumor size (P<0.001), alpha fetoprotein (AFP) (P=0.001), alanine aminotransferase (ALT) (P=0.024), and γ-glutamyl transferase (γ-GT) (P=0.024). However, SIRT4 was not an independent prognostic marker of HCC.

Conclusions. Our results demonstrated an association between SIRT4 expression levels, MVI, immune cell infiltration, and potential biological functions, including EMT in the progression of HCC.

Key words: Hepatocellular carcinoma, SIRT4, Microvascular infiltration, HCC progression, Invasion

Introduction

Hepatocellular carcinoma (HCC) is a common malignancy causing cancer death worldwide. The rates of HCC incidence and mortality are almost equivalent and have increased across most countries over the past three decades (Golabi et al., 2017; Martinez-Chantar et al., 2020; Soylu, 2020; McGlynn et al., 2021). Despite advances in medical, locoregional, and surgical therapies, patients with advanced HCC have few treatment options, and the prognosis is poor (Colecchia et al., 2014). Sirtuins are a conserved family of proteins that function as nicotinamide adenine dinucleotide (NAD+)-dependent deacetylases (Parihar et al., 2015). The sirtuin family consists of seven members (SIRT1-7) with different activities and functions. SIRT4/6 play a role in ADP-ribosylation, while others are pivotal for deacetylation (Carafa et al., 2012; Yamamoto et al., 2007). It was reported that the expression levels of SIRT4 were lower in cancer cells than in parallel normal cells, and SIRT4 overexpression inhibited cell

Corresponding Author: Shan Yu, MD, PhD, Department of Pathology, The Second Affiliated Hospital of Harbin Medical University, Harbin 150001, China. e-mail: yushan@hrbmu.edu.cn

www.hh.um.es. DOI: 10.14670/HH-18-794

Abbreviations. HCC, Hepatocellular carcinoma; NAD+, nicotinamide adenine dinucleotide; MVI, Microvascular infiltration; AFP, Alpha fetoprotein; ALT, Alanine aminotransferase; γ-GT, γ-glutamyl transferase; HCCDB, Database of Hepatocellular Carcinoma; LIHC, Liver hepatocellular carcinoma; DFS, Disease-free survival; OS, Overall survival; HR, Hazard ratio; CI, Confidence interval; TCA cycle, Tricarboxylic acid cycle; GDH, Glutamate dehydrogenase

proliferation and tumor development by repressing glutamine metabolism and promoting genomic stability (Carafa et al., 2012; Michan and Sinclair, 2007; Fernandez-Marcos and Serrano, 2013). These results suggest that SIRT4 serves as a tumor suppressor, inhibiting the progression of cancers. However, the tumor-suppressive function of SIRT4 in human cancers is not well studied, especially for prognostic marker value, association with immune cells and epithelial-mesenchymal transition (EMT), leading to further exploration of SIRT4's value in invasion or metastasis of liver cancer.

In the present study, we evaluated SIRT4 expression in HCC to elucidate the relationships between SIRT4 expression levels and progression, clinicopathological factors, immune cell infiltrations, and MVI (microvascular invasion) through EMT in HCC and to provide insights into SIRT4 functions, which could be a novel therapeutic strategy against HCC.

Materials and methods

Samples

A total of 108 patients with HCC who underwent curative resection were retrieved from the records of the Department of Pathology, the Second Affiliated Clinical College of Harbin Medical University, China, between January 2018 and April 2020. None of the patients received chemotherapy or radiotherapy before surgery. Thirty samples of adjacent normal liver tissue were obtained from the hepatectomy material around the HCC (more than 2 cm) and were used as controls. In our study, the original hematoxylin and eosin sections were reviewed by two independent pathologists, and specimens that were inadequate for consensus were not included. The following pathological diagnostic criterion was used for HCC: trabeculae with more than three cell thicknesses. Tumor cells may have eosinophilic, steatotic, or sometimes clear cytoplasms (Soylu, 2020). The maximum diameter of each HCC was recorded. MVI was defined as microscopic tumor invasion identified in the portal or hepatic vein of the surrounding liver tissue the liver tissue adjacent to the tumor (Cha et al., 2003). In doubtful cases, immunohistochemical analysis with CD34 was carried out to confirm the blood vessels (Portolani et al., 2014) (Table 1). Clinicopathological factors included sex, age, tumor size, hepatitis virus infection, cirrhosis, satellite nodules (defined as tumors <2 cm in size and located <2 cm from the main tumor) (Roayaie et al., 2009), alpha fetoprotein (AFP), alanine aminotransferase (ALT), γ-glutamyl transferase (γ-GT), and tumor differentiation. Tumor differentiation levels were defined as poor, moderate, and well according to the Edmondson-Steiner grading system.

Ethical statement

All the procedures for sample usage were approved by the Ethics Committee of Harbin Medical University, Second Affiliated Hospital (Approval No. KY2021-029), for experiments and complied with the 1964 Declaration of Helsinki and its later amendments or comparable ethical standards. All participants signed informed consent.

Pan-cancer analyses

The RNA-seq expression levels of SIRT4 were analyzed in TCGA pan-cancer database. Our analysis included 32 cancer types and 22 paired adjacent normal tissues among TCGA cohorts extracted from the Integrative Molecular Database of Hepatocellular Carcinoma (HCCDB), which contains 15 public HCC gene expression datasets with 3917 samples (Lian et al., 2018). The mean expression was calculated by Log2 (TPM+1). A scatter dot plot was plotted from the mean expression of both tumor and normal tissues.

Expression levels of SIRT4 from TCGA and validation cohorts

The RNA-seq expression data for liver hepatocellular carcinoma (LIHC) were extracted from TCGA through the GEPIA portal (Tang et al., 2017). These data included 160 normal liver samples (normal surgical samples adjacent to LIHC) and 369 LIHC samples. Adjacent normal liver tissue from TCGA cohort refers to liver tissue without liver cancer, which may be normal liver tissue, liver tissue with hepatitis or liver cirrhosis. A scatter dot plot was plotted from the RNA-seq expression: Log2 (TPM+1). The expression of SIRT4 in stage 1 to stage 4 LIHC was also plotted by a violin map with an F-test (Tang et al., 2017). For expression validation between HCC and adjacent tissue, we extracted data from the HCCDB with all validation cohorts, including 1, 3, 4, 6, 11, 12, 13, 15, 16, 17, and 18. A scatter plot was created. A p-value was calculated, and $p<0.05$ was considered statistically significant.

GO and KEGG analysis

The positively and negatively correlated genes with

Table 1. Detailed primary antibody information and dilutions.

Antibody	Clone	Dilution	Antigen retrieval	Incubation	Source
SIRT4	Ab231137	1:400	Citrate buffer	4°C, overnight	Abcam
CD34	QBEnd/10	1:100	EDTA	4°C, overnight	Thermo Fisher

SIRT4 expression were calculated by linkedomics, which uses Pearson correlation methods to display the top correlated genes in TCGA dataset in a heatmap (Vasaikar et al., 2018). The top 50 genes with positive and negative correlations with SIRT4 expression are displayed. Gene ontology (GO) and Kyoto Encyclopedia of Genes and Genomes (KEGG) analyses were carried out using positive and negative genes, respectively, with a cutoff at |0.3|. The up-to-date annotation versions of GO and KEGG (Kanehisa and Goto, 2000) analyses were run through the David bioinformatics website at v6.8 (Huang et al., 2009) and further plotted with R 3.5.2 software as previously described (Yu et al., 2019).

KM plot analysis

The survival times of patients with HCC were plotted by Kaplan-Meier analysis from GEPIA (both disease-free survival, DFS and overall survival, OS) and validated in the HCC cohort from the HCCDB (HCCDB6, HCCDB15, and HCCDB18) in both HCC samples and adjacent normal tissues. The median expression value was used as a cutoff point to separate patients into high- and low-expression groups. The patients at risk were also listed at each observed time point. A log-rank *P* value<0.5 was considered a positive prognostic marker of survival.

Correlation with Immune cell infiltration analysis.

The timer2.0 database was explored to calculate the association between immune cell infiltration and SIRT4 expression (Li et al., 2017). A spearman Rho test was used to demonstrate SIRT4 expression (log2 TPM) with the infiltration level in liver cancer. The TIMER method was the first choice, followed by CIBERSORT, MCPCOUNTER, and XCELL, if no data were displayed from the database. A *P*-value <0.05 was considered a positive association with the specific immune cell infiltration.

Immunohistochemical staining and grading

Immunohistochemical staining was performed on 5-μm-thick formalin-fixed, paraffin-embedded tissue sections. The antibodies, their source and dilution used in this study are shown in Table 1. Briefly, after sections were deparaffinized and dehydrated with xylene and ethanol, they were treated with Thermo Fisher peroxidase-blocking solution for 10 min at room temperature to block endogenous peroxidase activity. Antigen retrieval was performed and then incubation with a primary antibody using variable times and conditions (Table 1). EnVision™ detection reagent (Thermo Fisher) was used as a secondary antibody, 3'3-diaminobenzidine as a chromogen and hematoxylin as the counterstain. The appropriate positive and negative (primary antibody replaced by normal immunoglobulin) controls were processed simultaneously. All cases included adequate controls, negative controls, and internal controls. Control sections were processed without the primary antibodies and showed no positive signals. Normal liver tissue was the positive control.

Positive expression was defined by the presence of cytoplasmic and/or membranous reactivity in HCC cells. The evaluation of the cytoplasmic expression of SIRT4 corresponded with mitochondrial factors in the literature. A staining scoring system was evaluated by both staining intensity (weak=0, moderate=1, and strong=2) and staining area (<5%=0, 5%-25%=1, 25%-50%=2, 50%-75%=3, and >75%=4). The staining intensity score was computed, and the score of the staining area was the final staining score. SIRT4 expression was denoted as low expression (negative: 0-1 and weak: 2-4) and high expression (high: 5-7). The slides were examined by two experienced pathologists (Chen et al., 2011).

Evaluation of the degree of MVI

MVI was defined as the invasion of tumor cells in a portal vein, hepatic vein, or a large capsular vessel of the surrounding hepatic tissue, partially or totally lined with endothelial cells that were visible only upon microscopy (Hou et al., 2015). All patients were divided into three groups: M0 (number of invaded microvessels=0), M1 (1~5 proximal MVIs, ≤1 cm from the tumor boundary), and M2 (including >5 proximal MVIs, ≤1 cm from the tumor boundary) or (≥1 distal MVIs, >1 cm from the tumor boundary).

Correlation analysis of EMT markers

EMT is important for cancer metastasis. In liver cancer, EMT is associated with tumor initiation, invasion, and metastasis, further forming MVI. We performed EMT marker and immune checkpoint gene correlation analysis from TCGA database in liver cancer extracted from TIMER2.0 (Li et al., 2020). The Spearman rho value was calculated by the expression of SIRT4 by log2 TPM and major EMT genes including *CDH1*, *CDH2*, *VIM*, *MUC1*, *CTNNB1*, *ZEB1*, *MMP2*, *MMP9*, and *FN1*. Immune checkpoint genes (*CD274*, *PDCD1*, and *CTLA4*) were used.

Statistical analysis

The statistical calculations were performed using the SPSS 22.0 software package (SPSS Inc., China). Continuous variables are expressed as medians. The clinical and pathological differences between the study and control groups were evaluated using the Mann-Whitney two-sided U test for continuous data and the χ^2 test for categorical data (Fisher's exact test was used if the number of observations was <5). Statistical comparisons among the three groups were made using the Kruskal-Wallis test for nonparametric data. The OS differences between the two groups were evaluated with the Kaplan-Meier method and compared with the log-

rank test. Univariate and multivariate Cox proportional hazard regression analyses were performed to identify significant factors associated with OS. Survival indices of OS and progression-free survival (PFS) were expressed as hazard ratios (HRs) with 95% confidence intervals (95%CIs). The variables that were statistically significant by univariate analysis were included in a multivariate analysis. No interaction terms were considered because the pre-analysis showed no significance for the interaction. Data from these models were expressed as HR) and 95%CIs. All significance tests were two-sided, and differences were considered statistically significant with a *P*-value <0.05.

Results

SIRT4 is more highly expressed in HCC samples than in other cancers and normal tissues

In the present study, SIRT4 showed the highest RNA-seq levels in all solid tumors. The mean expression level in LIHC was 5.92, which was higher than that in any other cancer type, except AML (Acute Myeloid Leukemia). Compared with normal tissues, 13 (13/22) cancer types showed a lower SIRT4 level (Fig. 1A). In HCC, SIRT4 expression levels were higher in tumors than in normal tissues (Fig. 1B). However, in TCGA cohort of HCC, there were no significant changes in SIRT4 levels among the major stages (F value=0.402, Pr>F=0.752) (Fig. 1C). For the validation cohorts of HCC, the expression of SIRT4 in cancer tissues was higher than that in normal tissues in the HCCDB1, 3, 4, 6, 13, 15, 17, and 18 cohorts. In HCCDB11, 12, and 16, the *P*-value was >0.05, which may be explained by the limited patient number (<160) (Fig. 1D).

SIRT4 enhances mitochondrial function and is involved in cancer cell adhesion and migration

GO and KEGG analyses were performed to reveal the potential biological functions of SIRT4. The heatmap shows the top 50 positively or negatively related genes to SIRT4. As we separated positively and negatively correlated genes with SIRT4, the two heatmaps indicated the top 50 genes with SIRT4 (Fig. 2A). The KEGG-enrichment results also highlighted that SIRT4 widely participated in cancer-associated pathways, including the PI3K-AKT and TNF signaling pathways, due to the control of metabolic pathways (enriched results shown in Table 2, visualization in Fig. 2B).

SIRT4 is not an independent prognostic biomarker of HCC but is positively correlated with CD4+ T and NK cells and negatively with Cancer-associated fibroblasts.

The KM plot analysis of TCGA cohort of HCC suggested that SIRT4 was not a sensitive biomarker for clinical outcome prediction, including DFS and OS. In a cohort of 364 TCGA HCC patients, at the median expression cutoff value, the high vs. low SIRT4 group showed a log-rank *P*-value=0.2 in DFS (Fig. 3A). For OS, the high vs. low SIRT4 group showed a log-rank P-value=0.29 (Fig. 3B). Because of the high frequency of relapse in HCC, we only validated OS in the available HCCDB cohorts. There was a negative result when using SIRT4 as an independent prognostic biomarker in all three validation cohorts, including both tumor and adjacent tissues. In detail, the HCCDB6 cohort (n=225 HCC, n=220 adjacent tissue) had log-rank *P*-values of 0.32 and 0.264, respectively (Fig. 3C). For the HCCDB15 cohort (n=351 HCC, n=49 adjacent tissue), the log-rank *P*-values were 0.781 and 0.257, respectively (Fig. 3D). For the HCCDB18 validation cohort (n=212 HCC, n=177 adjacent tissue), the log-rank *P*-values were 0.243 and 0.159, respectively (Fig. 3E). As immune cells play an important role as regards survival and benefit from immune checkpoint inhibitor therapy, the association of the expression of SIRT4 with specific immune cell subtype infiltration was calculated with a Spearman Rho method (Fig. 4). For CD4+T cells, Rho=0.169 with a *P*-value=1.67e-3. For CD4+T cells, Rho=0.169 with a *P*-value=1.67e-3. For CD8+T cells, Rho=0.006 with a *P*-value=0.916. For Tregs cells, Rho=0.035 with a *P*-value=0.521. For B cells, Rho=0.032 with a *P*-value=0.548. For Monocyte cells, Rho=0.124 with a *P*-value=2.13e-2. For NK cells, Rho=0.137 with a *P*-value=1.08e-2. For Neutrophil cells, Rho=-0.013 with a *P*-value=0.809. For Macrophage cells, Rho=0.126 with a *P*-value=1.94e-2. For Myeloid dendritic cells, Rho=0.072 with a *P*-value=0.182. For Mast cells, Rho=0.113 with a *P*-value=3.57e-2. For cancer-associated fibroblast cells, Rho=-0.157 with a p-value=3.55e-3 (the results shown in Table 3).

Clinicopathological factors and histological factors in the cohort of 108 HCC patients

The details of the clinicopathological factors of the HCC patients used in this study are shown in Table 2. A total of 108 HCC patients, composed of 86 males and 22 females, were enrolled in the present study. The median age was 56.36 years (range 29-82 years). The median levels of AFP, ALT, and γ-GT were 15.46 ng/mL, 27.50 U/L, and 60.50 U/L, respectively. The rates of hepatitis and liver cirrhosis were 86.9% and 27.8%, respectively. Among the histopathological characteristics, the proportions of well, moderately, and poorly differentiated HCCs were 23.1%, 52.8%, and 24.1%, respectively.

Immunohistochemical expression pattern of SIRT4 in paired tumor and adjacent nonneoplastic liver tissues and clinicopathological factors

We observed that all adjacent non-neoplastic liver tissues and HCC samples showed a diffuse cytoplasmic expression pattern of SIRT4, with weak to strong

Table 2. GO (biological process and molecular function) and KEGG results.

	Count	*P*-Value	Fold Enrichment
Term GO BP positive			
GO:0006120~mitochondrial electron transport, NADH to ubiquinone	16	1.09E-15	19.79459
GO:0032981~mitochondrial respiratory chain complex I assembly	17	3.33E-15	16.35803
GO:0070125~mitochondrial translational elongation	16	7.58E-12	11.41100
GO:0070126~mitochondrial translational termination	16	9.05E-12	11.27831
GO:0006412~translation	19	2.11E-07	4.552561
GO:0043691~reverse cholesterol transport	7	2.94E-07	23.57481
GO:0034384~high-density lipoprotein particle clearance	5	1.04E-06	50.51745
GO:0033700~phospholipid efflux	6	2.05E-06	25.98040
GO:0033344~cholesterol efflux	7	2.54E-06	16.97386
GO:0034375~high-density lipoprotein particle remodeling	6	3.04E-06	24.24838
Term GO MF positive			
GO:0008137~NADH dehydrogenase (ubiquinone) activity	14	5.98E-13	17.58438
GO:0003735~structural constituent of ribosome	19	3.15E-08	5.159894
GO:0055102~lipase inhibitor activity	5	1.07E-06	50.24107
GO:0015485~cholesterol binding	7	5.34E-05	10.29329
GO:0060228~phosphatidylcholine-sterol O-acyltransferase activator activity	4	8.61E-05	40.19286
GO:0070653~high-density lipoprotein particle receptor binding	3	8.08E-04	60.28929
GO:0008289~lipid binding	9	0.00366	3.593401
GO:0008035~high-density lipoprotein particle binding	3	0.007136	22.60848
GO:0044822~poly(A) RNA binding	30	0.012192	1.602018
GO:0004532~exoribonuclease activity	3	0.021728	12.91913
Term GO BP negative			
GO:0045944~positive regulation of transcription from RNA polymerase II promoter	58	4.50E-09	2.314217
GO:0045893~positive regulation of transcription, DNA-templated	33	3.42E-06	2.508140
GO:0006468~protein phosphorylation	30	6.34E-06	2.575144
GO:0007163~establishment or maintenance of cell polarity	7	7.64E-05	9.448115
GO:0006366~transcription from RNA polymerase II promoter	29	1.37E-04	2.212716
GO:0001701~in utero embryonic development	15	3.21E-04	3.139748
GO:0035329~hippo signaling	6	5.34E-04	8.698265
GO:0098609~cell–cell adhesion	18	6.01E-04	2.599850
GO:0006351~transcription, DNA-templated	73	8.03E-04	1.461575
GO:0030335~positive regulation of cell migration	14	8.96E-04	2.978210
Term GO MF negative			
GO:0005515~protein binding	274	1.41E-06	1.215959
GO:0098641~cadherin binding involved in cell–cell adhesion	24	1.72E-06	3.226439
GO:0004674~protein serine/threonine kinase activity	27	4.72E-06	2.799537
GO:0046872~metal ion binding	84	1.79E-05	1.582811
GO:0004222~metalloendopeptidase activity	11	6.45E-04	3.795111
GO:0048365~Rac GTPase binding	6	0.003375	5.847921
GO:0005524~ATP binding	56	0.003922	1.460351
GO:0016874~ligase activity	16	0.004195	2.310290
GO:0003677~DNA binding	61	0.004601	1.420642
GO:0003779~actin binding	16	0.005465	2.243807
Term KEGG positive			
hsa00190:Oxidative phosphorylation	22	3.15E-14	8.686105
hsa05012:Parkinson's disease	22	1.21E-13	8.135577
hsa04932:Nonalcoholic fatty liver disease (NAFLD)	22	4.21E-13	7.650675
hsa05010:Alzheimer's disease	22	3.54E-12	6.876499
hsa05016:Huntington's disease	23	6.10E-12	6.290434
hsa01100:Metabolic pathways	48	3.32E-07	2.067719
hsa03010:Ribosome	11	2.32E-04	4.247250
hsa04975:Fat digestion and absorption	6	7.67E-04	8.078685
hsa03320:PPAR signaling pathway	6	0.008454	4.702518
hsa04122:Sulfur relay system	3	0.014441	15.75344
Term KEGG negative			
hsa04810:Regulation of actin cytoskeleton	20	2.43E-07	4.146474
hsa04510:Focal adhesion	18	3.92E-06	3.804289
hsa04151:PI3K-Akt signaling pathway	23	1.01E-05	2.902532
hsa04071:Sphingolipid signaling pathway	13	1.65E-05	4.716614
hsa05200:Pathways in cancer	24	2.52E-05	2.658808
hsa04668:TNF signaling pathway	12	2.89E-05	4.882764
hsa05205:Proteoglycans in cancer	16	4.65E-05	3.483038
hsa05222:Small cell lung cancer	10	1.25E-04	5.122115
hsa05215:Prostate cancer	10	1.64E-04	4.947497
hsa04611:Platelet activation	12	1.73E-04	4.018890

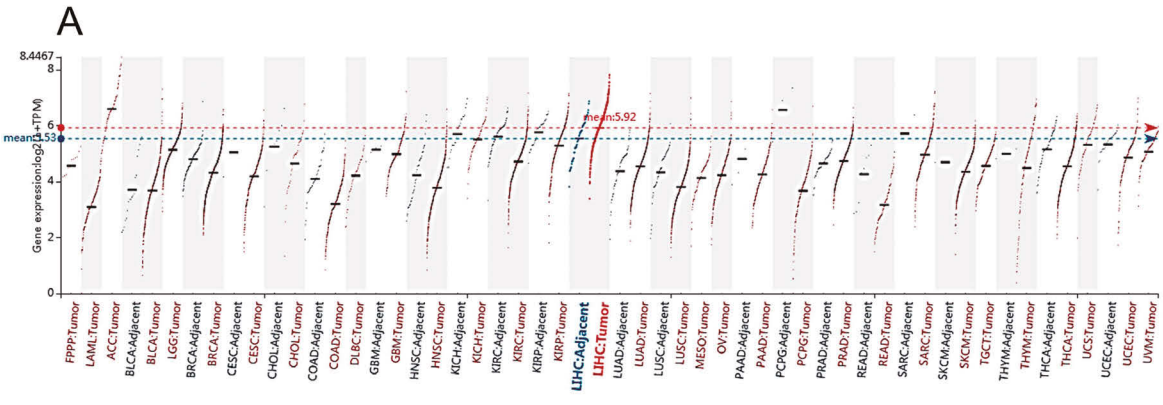

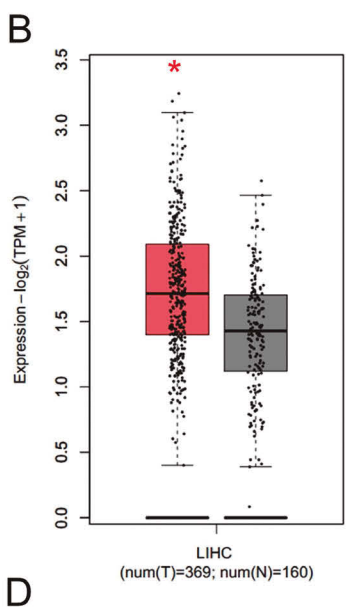

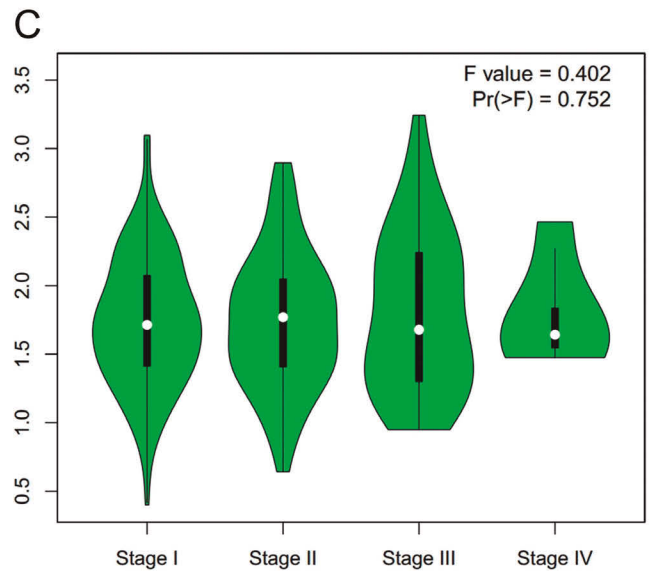

D

Dataset	P-value	Type	Nums	Mean
HCCDB1	1.170e-8	HCC	100	6.682
		Adjacent	97	6.148
HCCDB3	3.940e-20	HCC	268	0.1450
		Adjacent	243	0.09316
		Cirrhotic	40	0.05900
		Healthy	6	0.06900
HCCDB4	1.650e-17	HCC	240	6.582
		Adjacent	193	6.248
HCCDB6	3.080e-9	HCC	225	3.730
		Adjacent	220	3.605
HCCDB11	0.7816	HCC	88	6.297
		Adjacent	48	6.233
HCCDB12	0.4212	HCC	81	7.346
		Adjacent	80	7.429
HCCDB13	4.160e-19	HCC	228	4.872
		Adjacent	168	4.554
HCCDB15	0.0002850	HCC	351	5.964
		Adjacent	49	5.539
HCCDB16	0.09404	HCC	60	5.464
		Adjacent	60	5.534
HCCDB17	2.590e-7	HCC	115	7.556
		Adjacent	52	7.188
HCCDB18	2.590e-25	HCC	212	1.486
		Adjacent	177	1.024

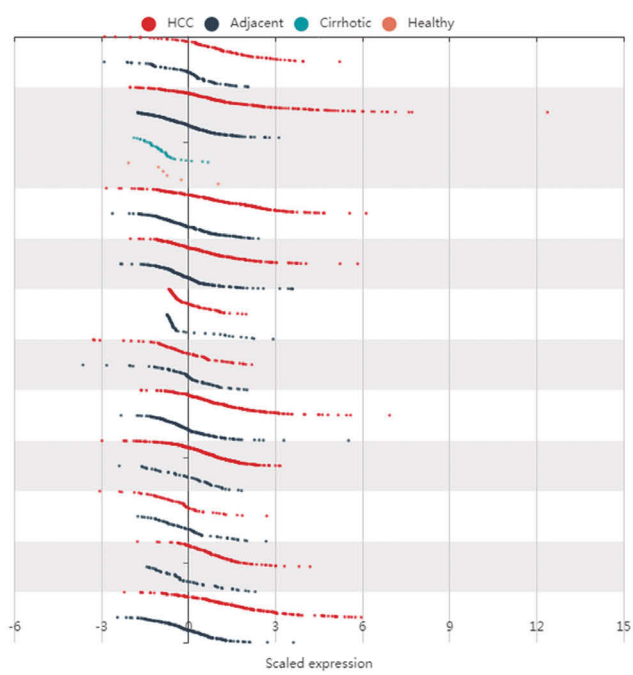

Fig. 1. A. Pan-cancer analysis of SIRT4 RNA-seq expression. TPM: transcripts per million. TCGA abbreviation list, LIHC: Liver hepatocellular carcinoma. Adjacent: Adjacent normal paired tissue. **B.** Expression difference of SIRT4 in T (tumor) and N (normal tissue). **C.** Violin plot of SIRT4 expression in LIHC from TCGA database with stage categories. **D.** Expression difference of SIRT4 in validation HCC cohorts in tumor samples and normal samples.

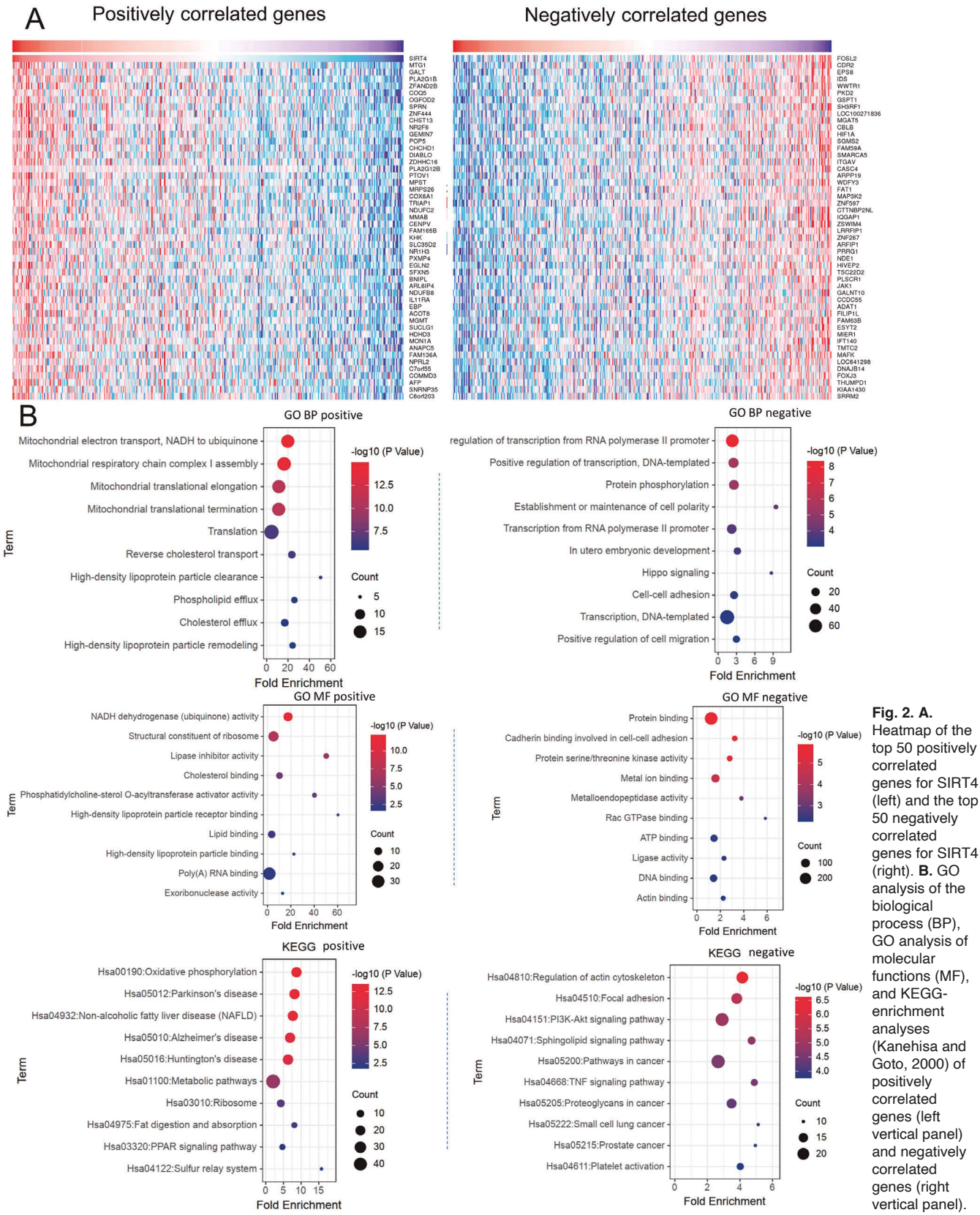

Fig. 2. A. Heatmap of the top 50 positively correlated genes for SIRT4 (left) and the top 50 negatively correlated genes for SIRT4 (right). **B.** GO analysis of the biological process (BP), GO analysis of molecular functions (MF), and KEGG-enrichment analyses (Kanehisa and Goto, 2000) of positively correlated genes (left vertical panel) and negatively correlated genes (right vertical panel).

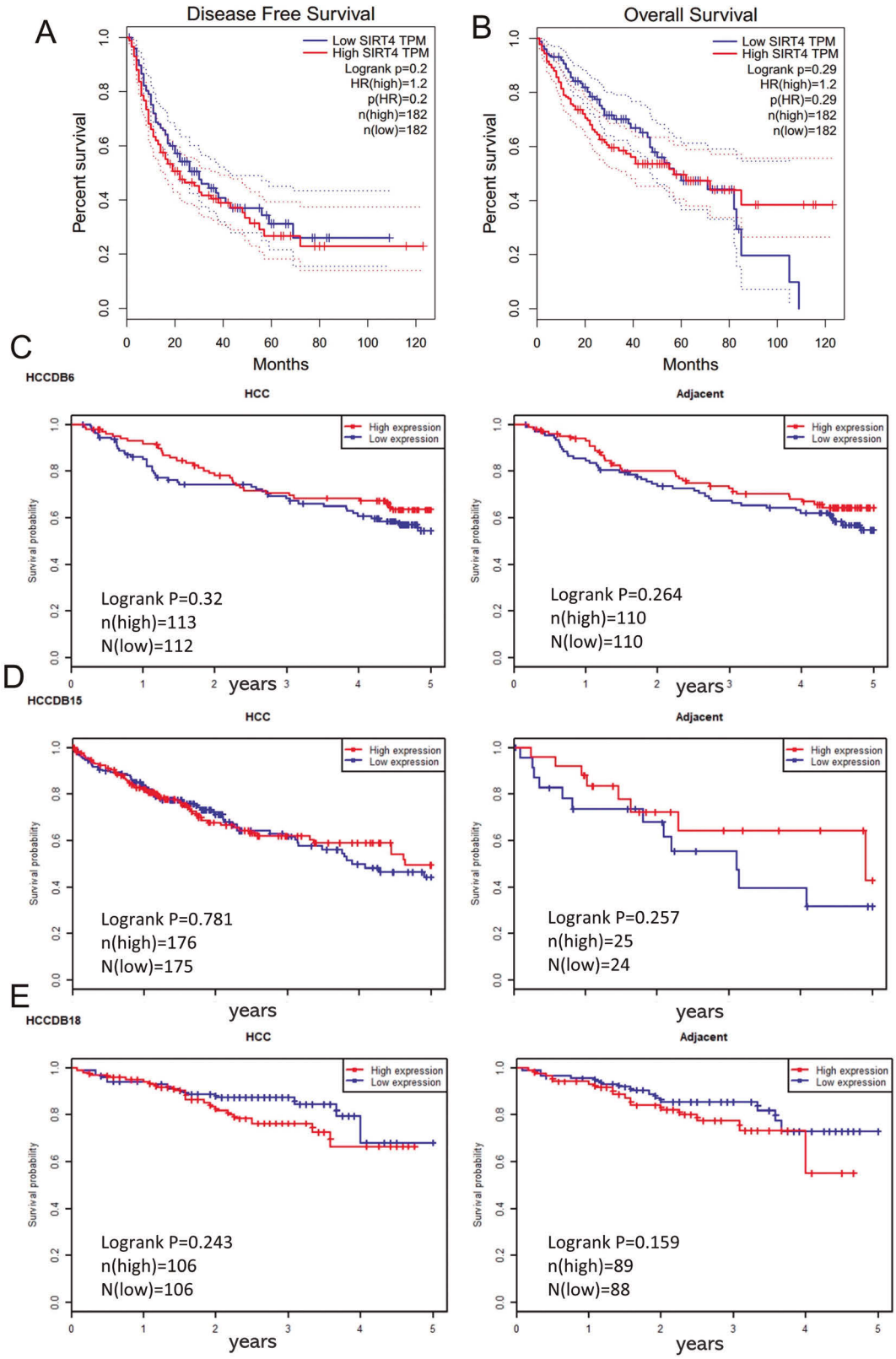

Fig. 3. A. Disease-free survival (DFS) KM plot of SIRT4 in the TCGA-LIHC cohort at the median cutoff by TPM (transcripts per million). HR=Hazard ratio. **B.** Overall survival (OS) KM plot of SIRT4 at the median cutoff by TPM. **C.** Validation KM plot (HCCDB6) of the overall KM plot at the median cutoff in both cancer and normal tissues. **D.** Validation cohort of HCCDB15 in OS. **E.** Validation cohort of HCCDB18 in OS.

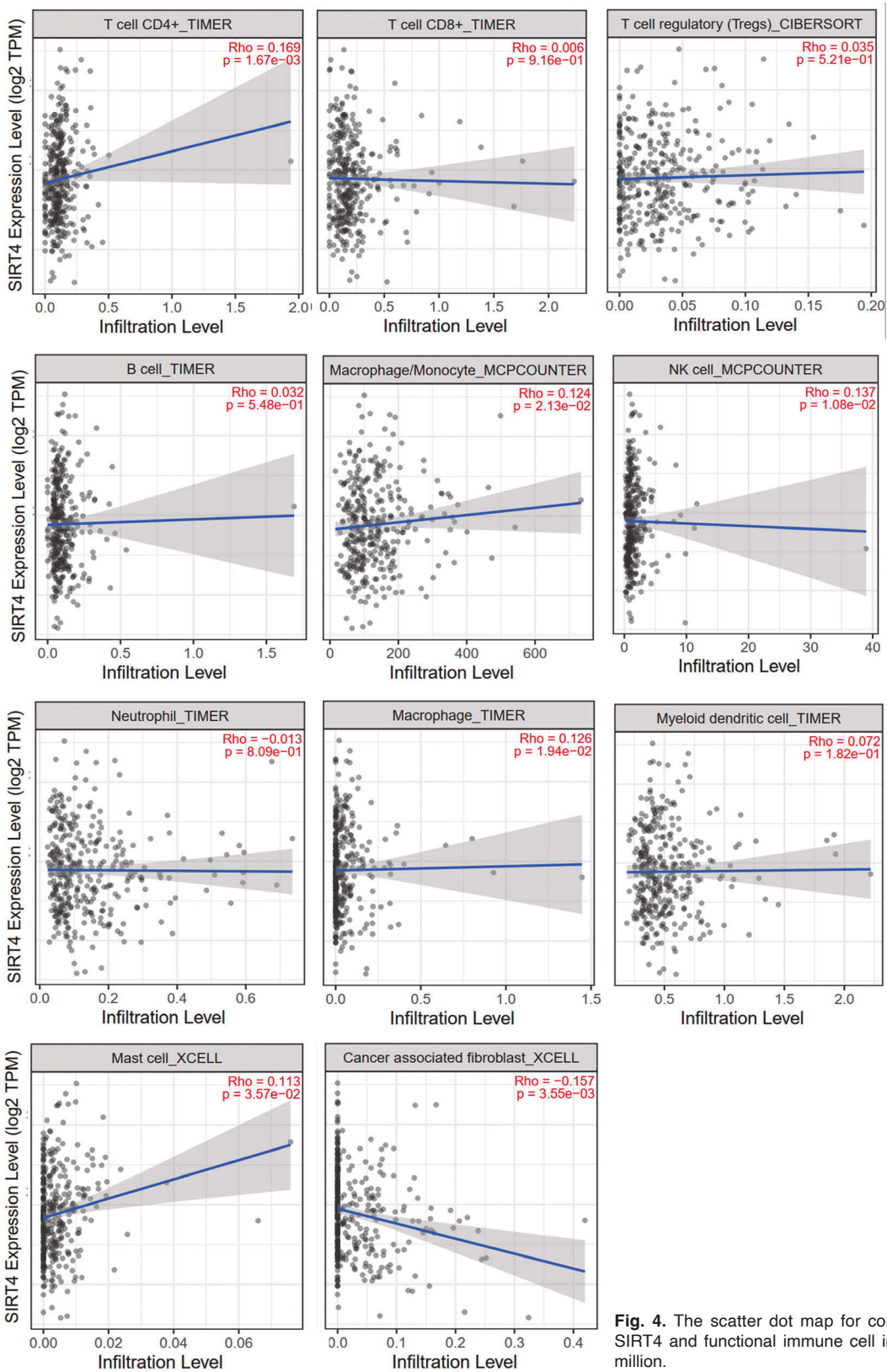

Fig. 4. The scatter dot map for correlation between expression of SIRT4 and functional immune cell infiltration. TPM= Transcripts per million.

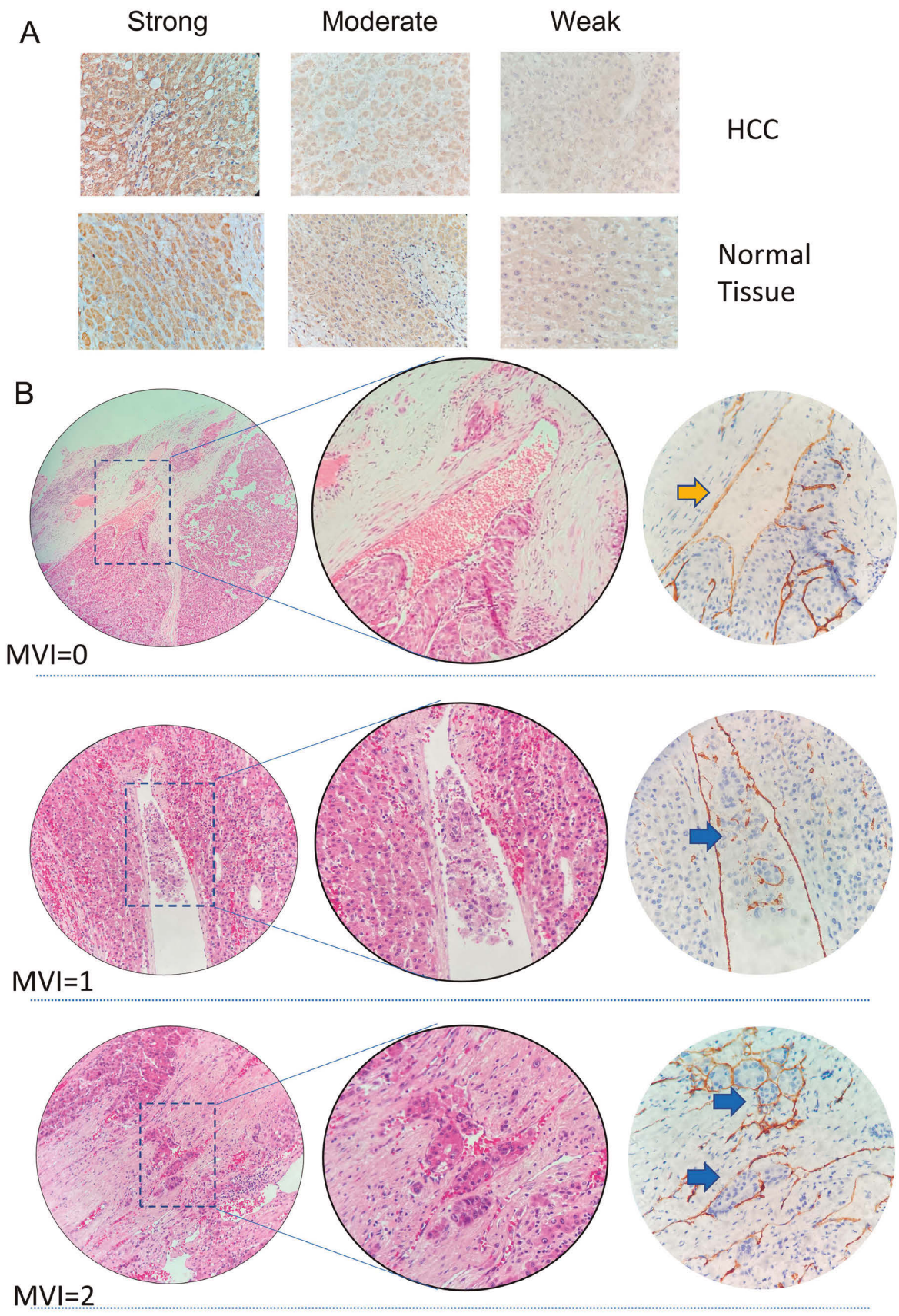

Fig. 5. A. Immunochemistry pattern of SIRT4 in HCC samples and adjacent normal tissue with staining intensity from strong to weak. **B.** Representative MVI IHC staining pattern. The blue arrows indicate CD34-positive blood vessels with cancer invasion. The yellow arrow indicates the blood vessel wall.

staining intensity (Fig. 5A). For normal liver tissue in our cohort, liver tissue with hepatitis, and liver cirrhosis, we analyzed the expression of SIRT4 and found no significant difference between different liver tissue statuses. To explore the clinical importance of SIRT4 expression in HCC, we analyzed the relationship between SIRT4 expression levels and clinicopathological factors. SIRT4 levels in either HCC tissues or adjacent non-neoplastic liver tissues did not correlate with sex, age, cell grade, tumor size, hepatitis virus infection, history of cirrhosis, satellite nodules, AFP levels, ALT levels, or γ-GT levels (Fig. 6A, Table 4).

Table 3. The association for of the expression of SIRT4 with specific immune cell subtype infiltration.

Cell type	Rho value=	A *p*-value
For CD4+T cells	0.169	=1.67e-3.
For CD4+T cells	0.169	=1.67e-3.
For CD8+T cells	0.006	=0.916.
For Tregs cells	0.035	=0.521.
For B cells	0.032	=0.548.
For Monocyte cells	0.124	=2.13e-2.
For NK cells	0.137	=1.08e-2.
For Neutrophil cells	-0.013	=0.809.
For Macrophage cells	0.126	=1.94e-2.
For Myeloid dendritic cells	0.072	=0.182.
For Mast cells	0.113	=3.57e-2.
For Cancer associated fibroblast cells	-0.157	=3.55e-3.

Correlation between microvascular invasion and clinicopathological factors with an explanation from EMT and immune checkpoint genes association.

The grade of MVI was defined as M0 (52 cases, 48.1%), M1 (34 cases, 31.5%), and M2 (22 cases, 20.4%). The expression level of SIRT4 was much lower in HCC tissues than in adjacent non-neoplastic liver tissues based on MVI being M1 or M2 (P=0.002) (Fig. 5B). Patients with lower SIRT4 levels displayed a higher MVI number.

Table 4. The correlation of clinicopathological factors and SIRT4 and MVI in HCC.

Characteristics	SIRT4 expression		*P*1 Value	MVI			*P*2 Value
	SIRT4 Low expression	SIRT4 High expression		M0	M1	M2	
Patients, Number (%)	51 (47.2)	57 (52.8)	0.335	52 (48.1)	34 (31.5)	22 (20.4)	0.551
Males, %	39 (76.5)	47 (82.5)		40 (76.9)	29 (85.3)	17 (77.3)	
Females, %	12 (23.5)	10 (17.5)		12 (23.1)	5 (14.7)	5 (22.7)	
Age, years (median)	55	56	0.898	57	54	56.5	0.431
Cell grade			0.710				0.258
Well differentiated(%)	10 (19.6)	15 (26.3)		20 (38.5)	5 (14.7)	0 (0)	0.003
Moderately differentiated(%)	28 (54.9)	29 (50.9)		20 (38.5)	22 (64.7	15 (68.2)	
Poorly differentiated(%)	13 (25.5)	13 (22.8)		12 (23.0)	7 (20.6)	7 (31.8)	
Size, cm (%)			0.193				<0.001
<3	13 (25.5)	19 (33.3)		21 (40.4)	7 (20.6)	4 (18.2)	
3-5	15 (29.4)	24 (42.1)		21 (40.4)	14 (41.2)	4 (18.2)	
5-10	19 (37.3)	9 (15.8)		7 (13.5)	13 (38.2)	8 (36.4)	
≥10	4 (7.8)	5 (8.8)		3 (5.7)	0 (0)	6 (27.2)	
Hepatitis virus infection			0.158				0.555
Yes(%)	42 (82.4)	52 (91.2)		47 (90.4)	29 (85.3)	18 (81.8)	
No(%)	9 (17.6)	5 (8.8)		5 (9.6)	5 (14.7)	4 (18.2)	
History of cirrhosis			0.943				0.216
Yes(%)	14 (27.5)	16 (28.1)		13 (25)	13 (38.2)	4 (18.2)	
No(%)	37 (72.5)	41 (71.9)		39 (75)	21 (61.8)	18 (81.8)	
Fatty change			0.855				0.394
Yes(%)	2 (16.7)	18 (18.7)		10 (50)	8 (40)	2 (10)	
No(%)	10 (83.3)	78 (81.3)		42 (47.7)	26 (29.6)	20 (22.7)	
Satellite nodule			0.608				0.254
Yes(%)	6 (11.8)	5 (8.8)		3 (5.8)	4 (11.8)	4 (18.2)	
No(%)	45 (88.2)	52 (91.2)		49 (94.2)	30 (88.2)	18 (81.8)	
Microvascular invasion (%)			0.003				
M0	16 (31.4)	36 (63.2)					
M1	21 (41.2)	13 (22.8)					
M2	14 (27.4)	8 (14.0)					
AFP	28.25	9.10	0.139	6.18	13.64	222.53	0.001
ALT	29.00	27.00	0.561	25.00	28.00	35.00	0.024
γ-GT	67.00	51.00	0.401	44.00	53.50	101.50	0.024

*P*1, significance of SIRT4 expression in HCC. *P*2, significance of MVI in HCC. The continuous parameters are described using median values.

Low SIRT4 expression was significantly (P=0.002) more commonly observed in M1 and M2 macrophages than in M0 macrophages (Fig. 6B). In addition, MVIs were closely related to cell grade (P=0.003), tumor size (P<0.001), AFP (P=0.001), ALT (P=0.024) and γ-GT (P=0.024) (Fig. 6C). However, there was no significant correlation between MVI and sex, age, hepatitis virus infection, history of cirrhosis, or satellite nodules. The clinical and histopathological data for all the patients in this study are summarized in Table 3. As the invasion of

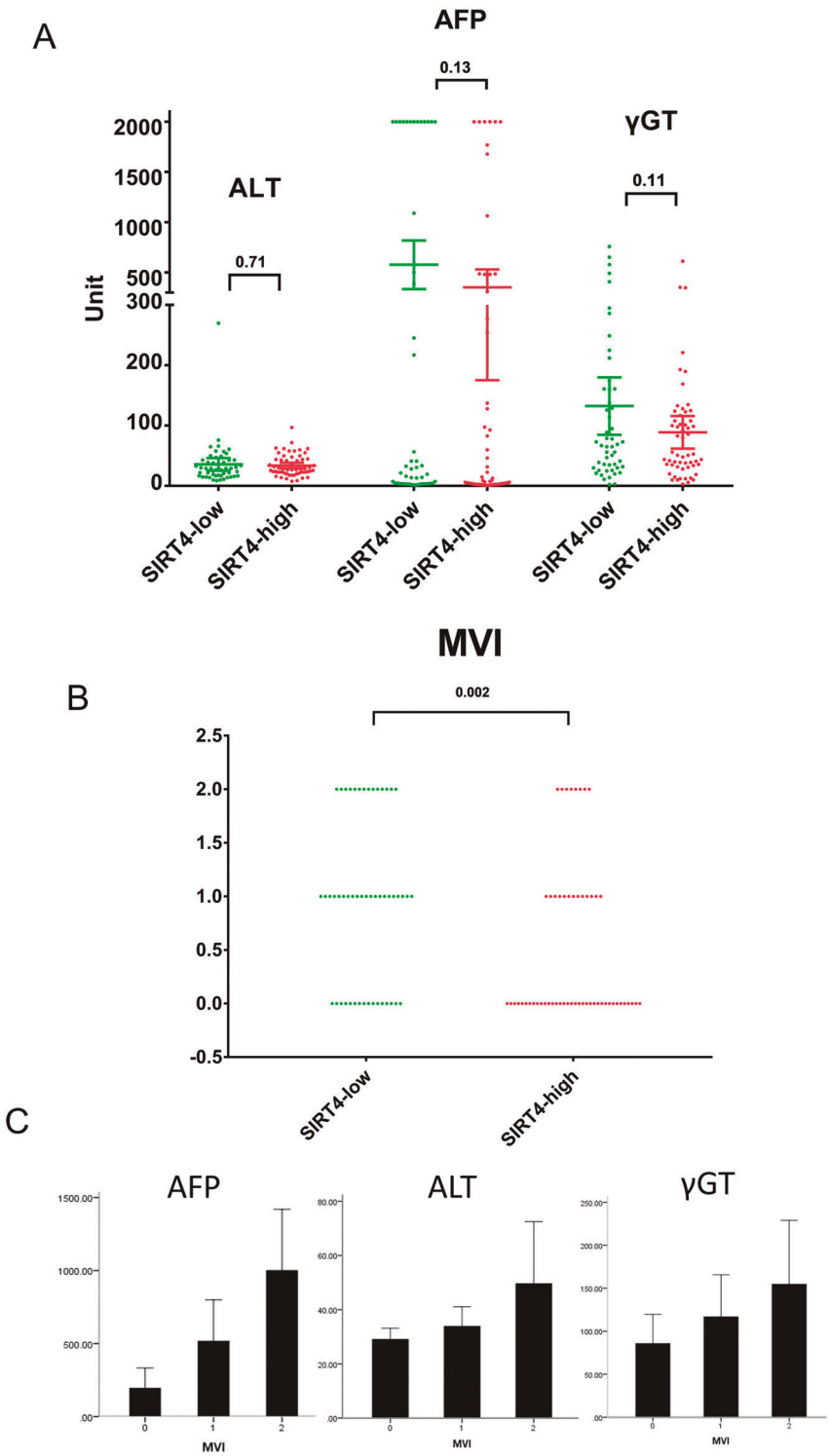

Fig. 6. A. Expression distribution of ALT, AFP, and γ-GT in the high and low SIRT4 groups. A P-value <0.05 was considered statistically significant. **B.** MVI score differences between the high and low SIRT4 groups. Low SIRT4 expression has a higher MVI score. **C.** The expression distribution of the clinical factors ALT, AFP, and γ-GT in different MVI groups.

cancer cells was mainly based on the EMT molecular mechanism, the EMT markers associated with SIRT4 expression were calculated to identify cell-cell adhesion capability regulated by SIRT4 (Fig. 7). The Rho for the correlation between CDH1 (E-cad) and SIRT4 was 0.028 (*P*-value=0.591) and for CDH2 (N-Cadherin), Rho=0.152 (*P*-value=3.43e-3). For Vim, Rho=-0.058 (*P*-value=2.64e-1). For MUC1 (EMA), Rho=-0.116 (*P*-value=2.53e-2). For CTNNB1 (beta-catenin), the Rho=0.228 (*P*-value=9.56e-6). For ZEB1, Rho=0.087 (*P*-value=9.31e-2). For MMP2, Rho=-0.09 (*P*-value=8.32e-2). For MMP9, Rho=-0.015 (*P*-value=0.77). For FN1, Rho=0.05 (*P*-value=0.334). For CD274(PD-L1), Rho=-0.002 (*P*-value=0.97). For PDCD1, Rho=0.032 (*P*-value=0.538). For CTLA4, Rho=0.022 (*P*-value=0.679) (the results shown in Table 5).

Discussion

The functions of SIRT4 and its expression are still controversial. Generally, SIRT4 has been proven to act as a tumor suppressor in many human cancers (Miyo et al., 2015). However, different reports exist, as SIRT4 is also upregulated in various malignancies by promoting tumor proliferation (Huang et al., 2017; Zhao et al., 2019). In liver cancer, silencing SIRT4 contributed to PPARδ signaling-mediated alternative activation of tumor-associated macrophages regulating HCC development (Li et al., 2019). Additionally, SIRT4 expression plays a tumor suppressor role in the induction of G2/M cell cycle arrest and apoptosis in hepatitis B virus-related HCC (Huang et al., 2021). However, that study mainly investigated the clinical significance and functional role of SIRT4 in HBV-related HCC. TCGA data analysis showed that SIRT4 expression was also lower in patients with HBV infection than in those without, and SIRT4 levels were positively associated with better patient survival. In our studies, TCGA data analysis included all HCC cases and ignored the HBV infection status. This phenomenon is of great interest in SIRT4 regulation under viral attack, which attracts our attention for further in-depth exploration by our research team. Regarding the protein expression of SIRT4 in HCC, there are many different results based on their study cohorts (Huang et al., 2016; Wang et al., 2019). According to our sample analysis results, HCC had relatively higher RNA-seq expression than other solid cancers. However, its prognostic value was not significant, as all KM analyses showed a negative statistical result. Our GO and KEGG analyses showed that SIRT4 mainly participated in mitochondrial translational functions, including energy transfer and metabolism, which are vital for regulating cancer cell adhesion and migration (regulation of the actin cytoskeleton). Biological function analysis revealed that SIRT4 primarily participated in mitochondrial energy metabolism, which displayed a connection with cell migration and adhesion. Notably, SIRT4 is involved in several classical cancer pathways, and its role in HCC still requires further investigation.

Table 5. The Rho value for the correlation between SIRT4 and EMT/immune check point markers.

Gene Name	Rho value=	A *P*-value
For CDH1	0.028	=0.591.
For CDH2	0.152	=3.43e-3.
For Vim	0.058	=2.64e-1.
For MUC1	0.116	=2.53e-2.
For CTNNB1	0.228	=9.56e-6.
For ZEB1	0.087	=9.31e-2.
For MMP2	0.090	=8.32e-2.
For MMP9	0.015	=0.770.
For FN1	0.050	=0.334.
For CD274	0.002	=0.970.
For PDCD1	0.032	=0.538.
For CTLA4	0.022	=0.679.

Our study explored the relationships between SIRT4 expression, MVI, and clinicopathological factors in HCC (The research flow chart is summarized in Fig. 8). The present data showed that all adjacent non-neoplastic liver tissues showed a diffuse cytoplasmic expression pattern of SIRT4, which is consistent with other studies (Miyo et al., 2015; Huang et al., 2015). Interestingly, the expression level of SIRT4 was significantly decreased in HCC tissues compared with adjacent non-neoplastic liver tissues based on MVI being M1 or M2 (P=0.003). This means that patients with lower SIRT4 levels possibly displayed a higher MVI number. In addition, there was a significant relationship between MVI and cell grade (P=0.003). The increasing MVI grade was significantly higher in large tumors than in small tumors (P<0.001). MVI numbers were higher in large tumors than in small tumors (P<0.001). This is consistent with the conclusion from Hui Zhao's study (Zhao et al., 2017). AFP, ALT, and γ-GT levels in M0 were significantly lower than in M1 and M2 (P=0.001, P=0.024, and P=0.024). These results were consistent with previous studies (Renzulli et al., 2016; Zhao et al., 2017).

According to the present study, SIRT4 is one of the least characterized sirtuins located in mitochondria. Unlike other sirtuins, SIRT4 has ADP-ribosyltransferase activity on histones instead of nicotinamide adenine dinucleotide-dependent deacetylase activity (Mahlknecht and Voelter-Mahlknecht, 2009). SIRT4 impairs entry of the tricarboxylic acid cycle (TCA cycle) by repressing glutamate dehydrogenase (GDH) to restrain glutamate into α-ketoglutarate. SIRT4 has tumor-suppressive effects, and its downregulation may facilitate the progression of human cancers (Haigis et al., 2006; Zhu et al., 2014; Csibi et al., 2021; Wang et al., 2021), including colorectal cancer, gastric adenocarcinoma, breast cancer, bladder cancer, ovarian cancer, and thyroid cancer. In addition, Jeong et al. added further evidence for SIRT4 in Myc-induced B-cell lymphoma, indicating its tumor suppressor role in both solid and nonsolid malignancies (Jeong et al., 2014). Studies on

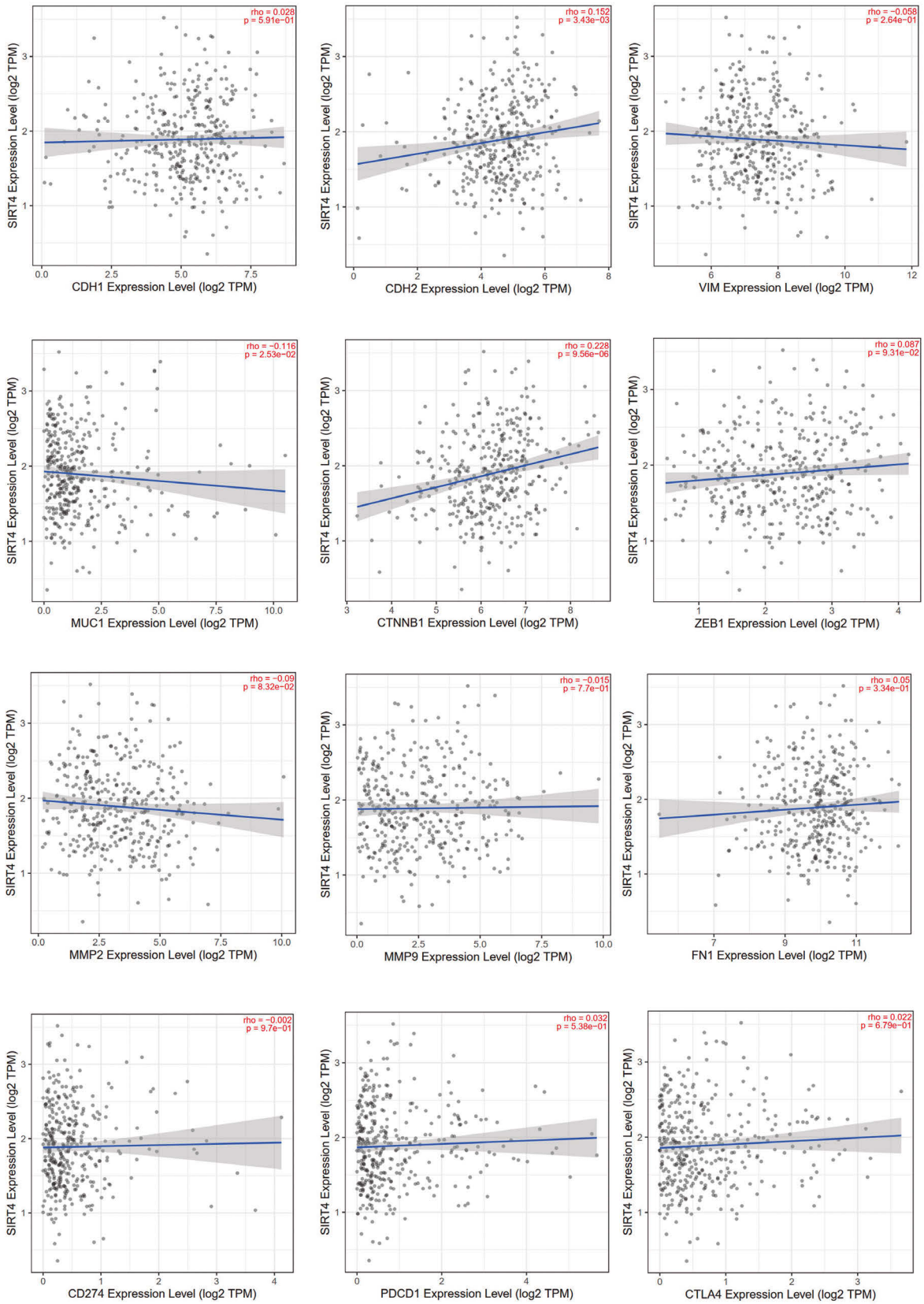

Fig. 7. The scatter dot map for correlation between expression of SIRT4 and EMT-related signature genes. TPM= Transcripts per million.

SIRT4 have increased in the last decade, but a paucity of studies have reported that overexpression of SIRT4 inhibits cell proliferation and tumor development. Seung Min Jeong showed that SIRT4 indeed plays an important role in the DNA damage response that orchestrates a metabolic block in glutamine metabolism, cell cycle arrest, and tumor suppression. SIRT4 loss leads to increased glutamine-dependent proliferation and stress-induced genomic instability, leading to tumorigenesis (Zhu et al., 2014). In the present study, we found that patients with lower SIRT4 expression levels have a higher risk of microvascular infiltration in HCC. Furthermore, it was shown that the novel risk classification of MVI based on histopathological features is valuable for predicting the prognosis of HCC patients after hepatectomy. HCC patients with MVI have a worse prognosis than HCC patients without MVI (Hirokawa et al., 2014; Iguchi et al., 2015; Shim et al., 2015; Rastogi, 2018; Forner et al., 2018). We also observed decreasing SIRT4 levels with increasing MVI grade (P<0.001). SIRT4 is a tumor suppressor gene, and the decrease or deletion of SIRT4 expression showed a statistically significant association with the increase in MVI grade. It also confirmed that the decrease or deletion of SIRT4 expression was related to the prognosis of HCC. Large well-designed studies with diverse populations and functional evaluations are warranted to confirm and extend our findings. The MVI-negative group showed a more favorable prognosis than the MVI-positive group. Compared with M0 patients, M1 and M2 patients experienced earlier recurrence and poor prognosis. In other words, MVI is an important factor that reflects the possibility of cancer cell metastasis. The decreased SIRT4 levels showed an increasing MVI index, suggesting that a higher SIRT4 expression level may strongly suppress the tumor metastasis process. Our results also highlighted that SIRT4 expression was correlated with EMT genes. SIRT4 expression is negatively correlated with *VIM*, *MMP2*, and *MUC1*, and positively correlated with *CDH2* and *CTNNB1*. These regulatory associations between SIRT4 and EMT genes may help us understand that SIRT4 is related to MVI. In addition, the changes in mitochondrial molecules may affect the structure and function of mitochondria, and studies have shown that mitochondrial dysfunction can increase the mobility and invasiveness of vascular cells (Han et al., 2021). It has been proven that SIRT4 dysfunction will affect vascular homeostasis (Kida and Goligorsky, 2016). So, we speculate that SIRT4 will affect the microvascular infiltration of liver cancer by affecting mitochondrial function, which requires further exploration and molecular mechanisms. Other explanations may exist, as SIRT4 expression levels are positively correlated with functional CD4+T cells, NK cells, mast cells, and cancer-associated fibroblasts. These immune cells may further contribute to the tumor suppressor role of SIRT4 in liver cancer from an immune response point of view. However, these findings are difficult to validate other than by using spacing transcriptome techniques combined with single-cell sequencing. Recent studies have shown that damaged mitochondria can disrupt physiological functions and may initiate injury signals through an inflammatory cascade (Harding et al., 2023). The possible signaling pathways are currently unclear. This requires further research.

In this study, we found a significant relationship between MVI and cell grade, tumor size, AFP, ALT, and γ-GT. Larger tumor sizes, higher levels of AFP, ALT, and γ-GT, and worse tumor differentiation were observed in the high MVI group compared with the non-MVI group in our study, which was consistent with

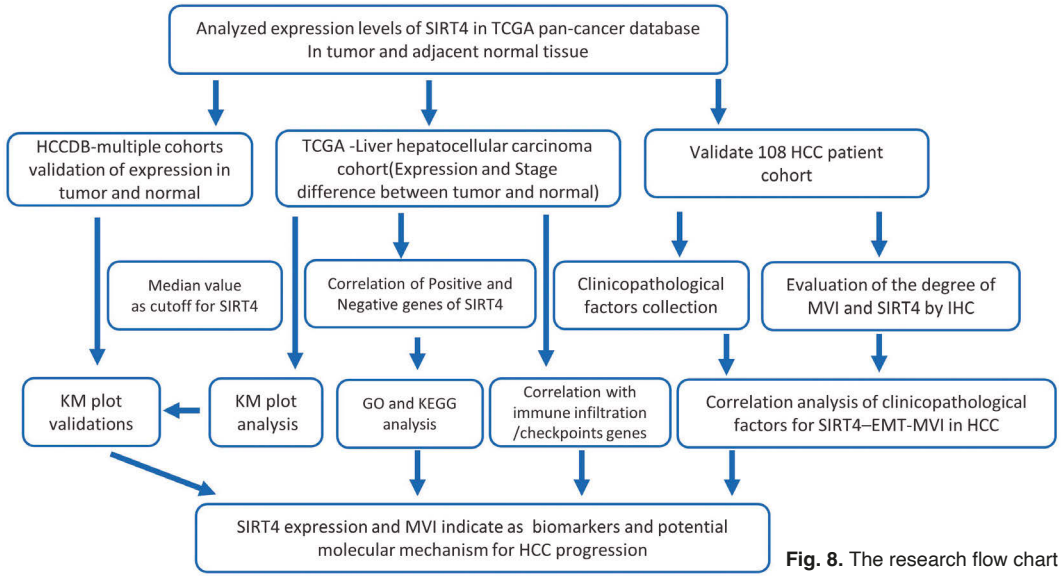

Fig. 8. The research flow chart of the present study.

previous studies (Yang et al., 2020). Generally, the prognosis of HCC with a larger size is inferior to that of HCC with a small size after curative resection because a large HCC is more frequently associated with adverse prognostic factors (Pawlik et al., 2005). It was reported that MVI and a tumor size >5 cm were independent risk factors for prognosis in patients with resected primary HCC (Hwang et al., 2015). Tumor size >5 cm was reported to be strongly related to the prevalence of MVI (Ahn et al., 2015). However, Yamashita et al. found that there was no significant correlation between tumor size and MVI. Thus, whether the prognosis of post-resection solitary HCC is independent of tumor size is controversial and needs further validation in clinical research (Yamashita et al., 2018).

In conclusion, our results suggest that SIRT4 expression and MVI may serve as valuable markers of HCC progression, and the EMT regulatory function of SIRT4 may warrant an in-depth study for a molecular explanation. SIRT4 has been studied in many diseases, however, a better understanding of its involvement in pathogenesis is required. There are limitations in the present study. The risk classification of MVI based on different histopathological characteristics needs to be validated in more patients. In our research, we support the result that SIRT4 may serve as a tumor suppressor in HCC, as high expression of SIRT4 reduced MVI numbers and correlated with CD4+T cells/NK cells and EMT genes, which may be explained by the regulation of mitochondrial energy metabolism and cell adhesion.

Acknowledgments and Funding. We thank the technicians in the pathology lab for their help with IHC staining. The study was funded by the National Natural Science Foundation of China: 81972724 to Sheng TAI.

Disclosure/Conflict of Interest. The authors declare no conflict of interest.

Author Contributions Statement. Juan Li and Ming Zhao wrote the main manuscript text and conducted the analysis. Weiwei Fan made the visualization of the data. Na Na performed the Immunohistochemistry experiment. Hui Chen helped with the statistical analysis. Ming Liang and Sheng Tai revised the manuscript. Shan Yu revised the manuscript and supervised the project. All authors reviewed and approved the manuscript.

Availability of Data and Materials. The datasets used and/or analyzed during the current study are available from the corresponding author upon reasonable request.

The databases include the Integrative Molecular Database of Hepatocellular Carcinoma (HCCDB) (http://lifeome.net/database/hccdb/home.html); GEPIA (http://gepia.cancer-pku.cn/index.html); LinkedOmics (http://linkedomics.org/login.php) (Accession Number: TCGA LIHC); TIMER2.0 (http://timer.cistrome.org/).

References

Ahn S.Y., Lee J.M., Joo I., Lee E.S., Lee S.J., Cheon J., Han J.K. and Choi B.I. (2015). Prediction of microvascular invasion of hepatocellular carcinoma using gadoxetic acid-enhanced MR and 18F-FDG PET/CT. Abdom. Imaging 40, 843-851.

Carafa V., Nebbioso A. and Altucci L. (2012). Sirtuins and disease: The road ahead. Front. Pharmacol. 3, 4.

Cha C., Fong Y., Jarnagin W.R., Blumgart L.H. and DeMatteo R.P. (2003). Predictors and patterns of recurrence after resection of hepatocellular carcinoma. J. Am. Coll. Surg. 197, 753-758.

Chen J., Zhang B., Wong N., Lo A.W.I., To K.-F., Chan A.W.H., Ng M.H.L., Ho C.Y.S., Cheng S.-H., Lai P.B.S., Yu J., Ng H.-K., Ling M.-T., Huang A.-L., Cai X.-F. and Ko B.C.B. (2011). Sirtuin 1 is upregulated in a subset of hepatocellular carcinomas where it is essential for telomere maintenance and tumor cell growth. Cancer Res. 71, 4138-4149.

Colecchia A., Schiumerini R., Cucchetti A., Cescon M., Taddia M., Marasco G. and Festi D. (2014). Prognostic factors for hepatocellular carcinoma recurrence. World J. Gastroenterol. 20, 5935-5950.

Csibi A., Fendt S.-M., Li C., Poulogiannis G., Choo A.Y., Chapski D.J., Jeong S.M., Dempsey J.M., Parkhitko A., Morrison T., Henske E.P., Haigis M.C., Cantley L.C., Stephanopoulos G., Yu J. and Blenis J. (2021). The mTORC1 pathway stimulates glutamine metabolism and cell proliferation by repressing SIRT4. Cell 184, 2256.

Fernandez-Marcos P.J. and Serrano M. (2013). Sirt4: The glutamine gatekeeper. Cancer Cell 23, 427-428.

Forner A., Reig M. and Bruix J. (2018). Hepatocellular carcinoma. Lancet 391, 1301-1314.

Golabi P., Fazel S., Otgonsuren M., Sayiner M., Locklear C.T. and Younossi Z.M. (2017). Mortality assessment of patients with hepatocellular carcinoma according to underlying disease and treatment modalities. Medicine 96, e5904.

Haigis M.C., Mostoslavsky R., Haigis K.M., Fahie K., Christodoulou D.C., Murphy A.J., Valenzuela D.M., Yancopoulos G.D., Karow M., Blander G., Wolberger C., Prolla T.A., Weindruch R., Alt F.W. and Guarente L. (2006). SIRT4 inhibits glutamate dehydrogenase and opposes the effects of calorie restriction in pancreatic beta cells. Cell 126, 941-954.

Han Y.S., Yi E.-Y., Jegal M.-E. and Kim Y.-J. (2021). Cancer stem-like phenotype of mitochondria dysfunctional Hep3B hepatocellular carcinoma cell line. Cells 10, 1608.

Harding O., Holzer E., Riley J.F., Martens S. and Holzbaur E.L.F. (2023). Damaged mitochondria recruit the effector NEMO to activate NF-κB signaling. Mol. Cell 83, 3188-3204.e7.

Hirokawa F., Hayashi M., Miyamoto Y., Asakuma M., Shimizu T., Komeda K., Inoue Y. and Uchiyama K. (2014). Outcomes and predictors of microvascular invasion of solitary hepatocellular carcinoma. Hepatol. Res. 44, 846-853.

Hou Y.-F., Li B., Wei Y.-G., Yang J.-Y., Wen T.-F., Xu M.-Q., Yan L.V.-N. and Chen K.-F. (2015). Second hepatectomy improves survival in patients with microvascular invasive hepatocellular carcinoma meeting the milan criteria. Medicine 94, e2070.

Huang D.W., Sherman B.T. and Lempicki R.A. (2009). Systematic and integrative analysis of large gene lists using DAVID bioinformatics resources. Nat. Protoc. 4, 44-57.

Huang G., Cui F., Yu F., Lu H., Zhang M., Tang H. and Peng Z. (2015). Sirtuin-4 (SIRT4) is downregulated and associated with some clinicopathological features in gastric adenocarcinoma. Biomed. Pharmacother. 72, 135-139.

Huang G., Lai X., Chen Z., Yu Z., Zhou D., Wang P., Zhou H. and Zhu G. (2016). Sirtuin-4 (SIRT4) is downregulated in hepatocellular carcinoma and associated with clinical stage. Int. J. Clin. Exp.

Pathol. 9, 6511-6517.
Huang G., Lin Y. and Zhu G. (2017). SIRT4 is upregulated in breast cancer and promotes the proliferation, migration and invasion of breast cancer cells. Int. J. Clin. Exp. Pathol. 10, 11849-11856.
Huang F.-Y., Wong D.K.-H., Seto W.-K., Mak L.-Y., Cheung T.-T. and Yuen M.-F. (2021). Tumor suppressive role of mitochondrial sirtuin 4 in induction of G2/M cell cycle arrest and apoptosis in hepatitis B virus-related hepatocellular carcinoma. Cell Death Discov. 7, 88.
Hwang S., Lee Y.-J., Kim K.-H., Ahn C.-S., Moon D.-B., Ha T.-Y., Song G.-W., Jung D.-H. and Lee S.-G. (2015). The impact of tumor size on long-term survival outcomes after resection of solitary hepatocellular carcinoma: Single-institution experience with 2558 patients. J. Gastrointest. Surg. 19, 1281-1290.
Iguchi T., Shirabe K., Aishima S., Wang H., Fujita N., Ninomiya M., Yamashita Y.-i., Ikegami T., Uchiyama H., Yoshizumi T., Oda Y. and Maehara Y. (2015). New pathologic stratification of microvascular invasion in hepatocellular carcinoma: Predicting prognosis after living-donor liver transplantation. Transplantation 99, 1236-1242.
Jeong S.M., Lee A., Lee J. and Haigis M.C. (2014). SIRT4 protein suppresses tumor formation in genetic models of Myc-induced B cell lymphoma. J. Biol. Chem. 289, 4135-4144.
Kanehisa M. and Goto S. (2000). KEGG: Kyoto encyclopedia of genes and genomes. Nucleic Acids Res. 28, 27-30.
Kida Y. and Goligorsky M.S. (2016). Sirtuins, cell senescence, and vascular aging. Can. J. Cardiol. 32, 634-641.
Li T., Fan J., Wang B., Traugh N., Chen Q., Liu J.S., Li B. and Liu X.S. (2017). TIMER: A web server for comprehensive analysis of tumor-infiltrating immune cells. Cancer Res. 77, e108-e110.
Li Z., Li H., Zhao Z.-B., Zhu W., Feng P.-P., Zhu X.-W. and Gong J.-P. (2019). SIRT4 silencing in tumor-associated macrophages promotes HCC development via PPARδ signalling-mediated alternative activation of macrophages. J. Exp. Clin. Cancer Res. 38, 469.
Li T., Fu J., Zeng Z., Cohen D., Li J., Chen Q., Li B. and Liu X.S. (2020). TIMER2.0 for analysis of tumor-infiltrating immune cells. Nucleic Acids Res. 48, W509-W514.
Lian Q., Wang S., Zhang G., Wang D., Luo G., Tang J., Chen L. and Gu J. (2018). HCCDB: A database of hepatocellular carcinoma expression atlas. Genomics Proteomics Bioinformatics 16, 269 -275.
Mahlknecht U. and Voelter-Mahlknecht S. (2009). Fluorescence *in situ* hybridization and chromosomal organization of the sirtuin 4 gene (Sirt4) in the mouse. Biochem. Biophys. Res. Commun. 382, 685-690.
Martinez-Chantar M.L., Avila M.A. and Lu S.C. (2020). Hepatocellular carcinoma: Updates in pathogenesis, detection and treatment. Cancers 12, 2729.
McGlynn K.A., Petrick J.L. and El-Serag H.B. (2021). Epidemiology of hepatocellular carcinoma. Hepatology 73 (Suppl .1), 4-13.
Michan S. and Sinclair D. (2007). Sirtuins in mammals: Insights into their biological function. Biochem. J. 404, 1-13.
Miyo M., Yamamoto H., Konno M., Colvin H., Nishida N., Koseki J., Kawamoto K., Ogawa H., Hamabe A., Uemura M., Nishimura J., Hata T., Takemasa I., Mizushima T., Doki Y., Mori M. and Ishii H. (2015). Tumour-suppressive function of SIRT4 in human colorectal cancer. Br. J. Cancer 113, 492-499.
Parihar P., Solanki I., Mansuri M.L. and Parihar M.S. (2015). Mitochondrial sirtuins: Emerging roles in metabolic regulations, energy homeostasis and diseases. Exp. Gerontol. 61, 130-141.
Pawlik T.M., Delman K.A., Vauthey J.N., Nagorney D.M., Ng I.O.-L., Ikai I., Yamaoka Y., Belghiti J., Lauwers G.Y., Poon R.T. and Abdalla E.K. (2005). Tumor size predicts vascular invasion and histologic grade: Implications for selection of surgical treatment for hepatocellular carcinoma. Liver Transpl. 2005. 11, 1086-1092.
Portolani N., Baiocchi G.L., Molfino S., Benetti A., Gheza F. and Giulini S.M. (2014). Microvascular infiltration has limited clinical value for treatment and prognosis in hepatocellular carcinoma. World J. Surg. 38, 1769-1776.
Rastogi A. (2018). Changing role of histopathology in the diagnosis and management of hepatocellular carcinoma. World J. Gastroenterol. 24, 4000-4013.
Renzulli M., Brocchi S., Cucchetti A., Mazzotti F., Mosconi C., Sportoletti C., Brandi G., Pinna A.D. and Golfieri R. (2016). Can current preoperative imaging be used to detect microvascular invasion of hepatocellular carcinoma? Radiology 279, 432-442.
Roayaie S., Blume I.N., Thung S.N., Guido M., Fiel M.-I., Hiotis S., Labow D.M., Llovet J.M. and Schwartz M.E. (2009). A system of classifying microvascular invasion to predict outcome after resection in patients with hepatocellular carcinoma. Gastroenterology 137, 850-855.
Shim J.H., Jun M.-J., Han S., Lee Y.-J., Lee S.-G., Kim K.M., Lim Y.-S. and Lee H.C. (2015). Prognostic nomograms for prediction of recurrence and survival after curative liver resection for hepatocellular carcinoma. Ann. Surg. 261, 939-946.
Soylu N.K. (2020). Update on hepatocellular carcinoma: A brief review from pathologist standpoint. J. Gastrointest. Cancer 51, 1176-1186.
Tang Z., Li C., Kang B., Gao G., Li C. and Zhang Z. (2017). GEPIA: A web server for cancer and normal gene expression profiling and interactive analyses. Nucleic Acids Res. 45(W1), W98-W102.
Vasaikar S.V., Straub P., Wang J. and Zhang B. (2018). LinkedOmics: Analyzing multi-omics data within and across 32 cancer types. Nucleic Acids Res. 46, D956-D963.
Wang Y., Du L., Liang X., Meng P., Bi L., Wang Y.-L., Wang C. and Tang B. (2018). Sirtuin 4 depletion promotes HCC tumorigenesis through regulating adenosine-monophosphate-activated protein kinase alpha/mammalian target of Rapamycin axis in mice. Hepatology 69, 1614-1631.
Wang H., Li J., Huang R., Fang L. and Yu S. (2021). SIRT4 and SIRT6 serve as novel prognostic biomarkers with competitive functions in serous ovarian cancer. Front. Genet. 12, 666630.
Yamamoto H., Schoonjans K. and Auwerx J. (2007). Sirtuin functions in health and disease. Mol. Endocrinol. 21, 1745-1755.
Yamashita Y.-i., Imai K., Yusa T., Nakao Y., Kitano Y., Nakagawa S., Okabe H., Chikamoto A., Ishiko T., Yoshizumi T., Aishima S., Maehara Y. and Baba H. (2018). Microvascular invasion of single small hepatocellular carcinoma ≤3 cm: Predictors and optimal treatments. Ann. Gastroenterol. Surg. 2, 197-203.
Yang C., Huang X., Liu Z., Qin W. and Wang C. (2020). Metabolism-associated molecular classification of hepatocellular carcinoma. Mol. Oncol. 14, 896-913.
Yu S., Jiang X., Li J., Li C., Guo M., Ye F., Zhang M., Jiao Y. and Guo B. (2019). Comprehensive analysis of the GATA transcription factor gene family in breast carcinoma using gene microarrays, online databases and integrated bioinformatics. Sci. Rep. 9, 4467.
Zhao H., Chen C., Fu X., Yan X., Jia W., Mao L., Jin H. and Qiu Y. (2017). Prognostic value of a novel risk classification of microvascular invasion in patients with hepatocellular carcinoma after resection. Oncotarget 8, 5474-5486.
Zhao E., Hou J., Ke X., Abbas M.N., Kausar S., Zhang L. and Cui H.

(2019). The roles of sirtuin family proteins in cancer progression. Cancers 11, 1949.

Zhu Y., Yan Y., Principe D.R., Zou X., Vassilopoulos A. and Gius D. (2014). SIRT3 and SIRT4 are mitochondrial tumor suppressor proteins that connect mitochondrial metabolism and carcinogenesis. Cancer Metab. 2, 15.

Accepted July 12, 2024